ARCHIVES
of
FOUNDRY ENGINEERING

ISSN (2299-2944)

10.24425/afe.2025.155368

Published quarterly as the organ of the Foundry Commission of the Polish Academy of Sciences

Influence of Chemical Composition on Concentration Undercooling of Structural Steels

Y. Aftandiliants [a, b], S. Gnyloskurenko [a, b, *], H. Meniailo [b], V. Khrychikov [b]
[a] Physical and Technological Institute of Metals and Alloys, National Academy of Sciences of Ukraine, Ukraine
[b] National University of Life and Environmental Sciences of Ukraine, Ukraine
* Corresponding author: E-mail address: slava.vgn@gmail.com

Received 05.10.2024; accepted in revised form 12.03.2025; available online 12.09.2025

Abstract

The article studies the undercooling of steel melt around the solid particles, which is one of the main factors determining the rates of nucleation and growth of crystallization centers. Particularly, the effect of chemical composition on this factor for two grades structural cast steels 20KhGSL and 40Kh3G3S3L mainly containing Cr, Mn, Si was in the focus. The established analytical dependence allowed to determine the development of maximum concentration undercooling over the moving crystallization front depending on the liquidus temperature, the content of elements in the melt, their distribution and diffusion coefficients, the crystallization rate and the temperature gradient in the melt ahead the crystallization front. The correlation of maximum concentration undercooling and width of the columnar dendrite zone was obtained. The effect of chemical composition on steels undercooling and crystallization process was revealed. The efficiency of the elements influence changes for steels 20KhGSL and 40Kh3G3S3L from 20.1 to 25.9% for C, from 31.2 to 25.9% for Si, from 3.8 to 18.0% for Mn, from 34.0 to 10.8% for Cr, from 6.6 to 5.6% for S, from 1.0 to 0.4% for P, from 3.3 to 6.2% for N, respectively. The results obtained give deep insight in obtaining high quality steels.

Keywords: Steel, Chemical composition, Melt, Concentration undercooling, Distribution coefficient, Diffusion, Crystallization rate, Temperature gradient

1. Introduction

It is known [1-4] that the formation of the primary structure during steel solidification is determined by the regularities of nucleation and growth of crystallization centers.

The fundamental equations of the analytical description of homogeneous and heterogeneous nucleation rate of crystallization centers [5], as well as their growth during the formation of two-dimensional nuclei on the surface of a growing crystal [6, 7] with the presence of dislocations in the crystal [7, 8] and continuous growth [9] includes as a main parameter the undercooling around crystallization centers (ΔT). It depends on concentration undercooling (ΔT_c) and thermophysical conditions of solidification (ΔT_{tph}), which are related to the liquidus temperature (T_l), melt density (ρ_l) and surface tension between the melt and the crystal ($\sigma_{l\text{-}s}$) by the following dependence [10].

$$\Delta T = \Delta T_{tph} + \Delta T_c = \frac{\sigma_{l\text{-}s} \cdot T_l}{r \cdot \rho_l \cdot q_{cr}} + \Delta T_c, \quad (1)$$

where r – radius of the crystallization center; q_{cr} – specific heat of crystallization.

In pure metals, the undercooling of the melt is determined only by the thermophysical conditions of solidification (ΔT_{tph}), whereas in alloys, concentration undercooling (ΔT_c) additionally occurs due to their chemical composition.

The composition of solid phase differs from the composition of the melt from which it was formed. This leads to the appearance of a concentration gradient in the melt ahead of the crystallization front. If the solubility of a chemical element (C) in the solid phase is less than in the melt (C_0) from which the solid phase is formed, then the chemical element accumulates in the melt in front of the crystallization front. In the case when during the solidification there is not enough time for a uniform distribution of chemical elements over the volume of the remaining melt, the concentration gradient appears before the crystallization front and is maintained during the crystallization process, which leads to the occurrence of concentration undercooling.

The distribution of the chemical element in front of the moving crystallization front is shown in Fig. 1 a.

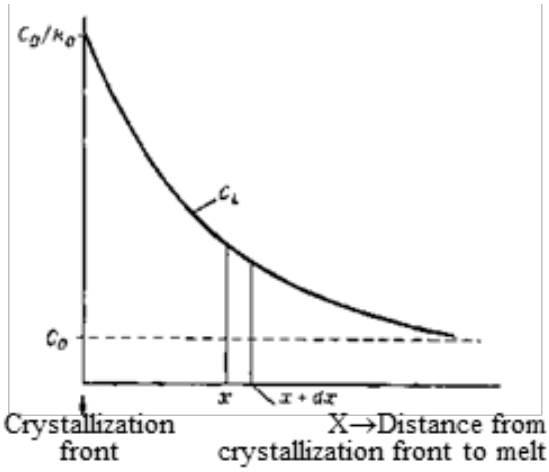

a

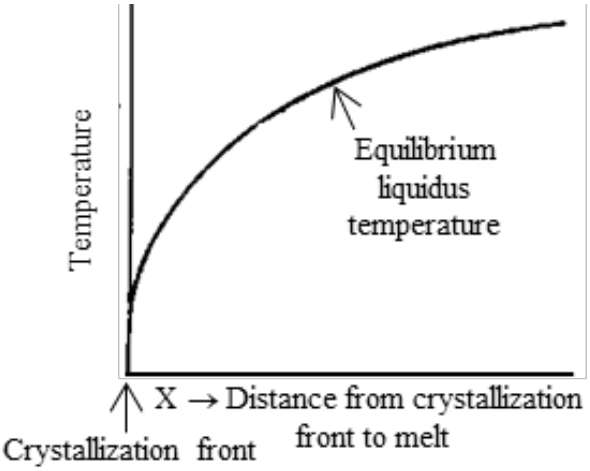

b

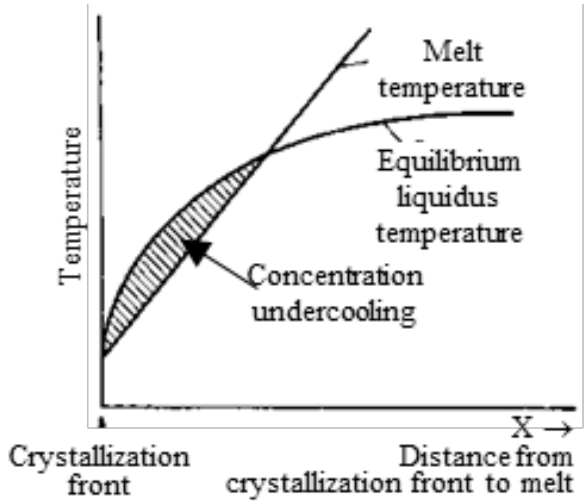

c

Fig. 1. Distribution of the chemical element (a) and liquidus temperature (b) ahead of the moving crystallization front and the development of concentration undercooling (c) [11]

The concentration of the chemical element C at the crystallization front reaches its maximum value on the surface of the crystals (C_0/k_0, where k_0 is the equilibrium distribution coefficient of the chemical element (C)) and decreases exponentially with the distance from the crystallization front to the value C_0 (Fig. 1 a). The nature of the distribution of chemical elements before the crystallization front is determined by the rate of their removal from the crystallization front into the melt and the process of their accumulation along the crystallization front. The removal rate is determined by chemical elements diffusion coefficient in the melt (D) and the process of their accumulation is determined by the rate of crystallization front movement (R). In the case when the quantity of elements that accumulate in front of the crystallization front per unit time is equal to the quantity of elements that diffuse from the crystallization front into the liquid phase the stationary regime is established, described by the following dependence [11]:

$$D\left(\frac{\partial^2 c}{\partial x^2}\right)+R\left(\frac{\partial c}{\partial x}\right)=0, \tag{2}$$

where x is the distance from the selected point in the melt to the crystallization front.

The solution to this equation has the form [11]

$$C_L = C_0\left(1+\frac{1-k_0}{k_0}e^{-\frac{R}{D}x}\right), \tag{3}$$

where C_L is the concentration of the chemical element of the melt at point x; C_0 is the initial concentration of the chemical element in the melt.

At large values of x, concentration $C_L = C_0$. At $x = 0$, $C_L = C_0/k_0$ (Fig. 1 a).

Simultaneously with the accumulation of chemical elements ahead of the moving crystallization front, the liquidus temperature changes in this zone. The influence of elements on the liquidus temperature of the melt is determined by the following expression:

$$T_L = T_0 - mC_L, \tag{4}$$

where T_L — liquidus temperature of the melt with composition C_L; T_0 is the crystallization temperature of pure metal; m is the slope of the liquidus line.

Considering Equation 3

$$T_L = T_0 - mC_0\left(1+\frac{1-k_0}{k_0}e^{-\frac{R}{D}x}\right), \tag{5}$$

The distribution curve of a chemical element in the melt, which is described by equation (3), and the equilibrium liquidus temperature curve, which is described by equation (5), are schematically presented in Fig. 1 (a and b, respectively).

The surface temperature of the crystallization front (T_{sf}) corresponds to the equilibrium liquidus temperature for the liquid located on the crystallization front in a stationary mode and is determined by Equation (6).

$$T_{sf} = T_0 - \frac{mC_0}{k_0}, \tag{6}$$

The temperature of an arbitrary point x in the melt (T) can be set with using the (7)

$$T = T_{sf} + G_L x, \tag{7}$$

where G_L — temperature gradient in the melt.

Taking into account equation 6, we can write

$$T = T_0 - \frac{mC_0}{k_0} + G_L x, \tag{8}$$

When the temperature (T) graph **crosses** the liquidus equilibrium temperature curve shown in Fig. 1 c, it is clear that some part of the liquid before the crystallization front has a temperature lower than its liquidus temperature, which indicates that developed the concentration undercooling.

The criterion for the occurrence of concentration undercooling is the ratio of the temperature gradient in the melt (G_L) to the crystallization rate (R), which is realized under the following condition [11].

$$\frac{G_L}{R} \geq \frac{mC_0(1-k_0)}{k_0 D}, \tag{9}$$

The extent of the zone of concentration undercooling is determined as the value of $\boldsymbol{x}$, at $T_L = T$, according to the following equation [11]:

$$1-\exp\left(-\frac{R\cdot x}{D}\right)=\frac{G_L\cdot k_0\cdot x}{mC_0(1-k_0)}, \tag{10}$$

The influence of the rate of movement of the crystallization front (R) and the temperature gradient in the melt (G_L) on the extent of the zone of concentration undercooling at different values of the liquidus temperature is shown in Fig. 2 [12].

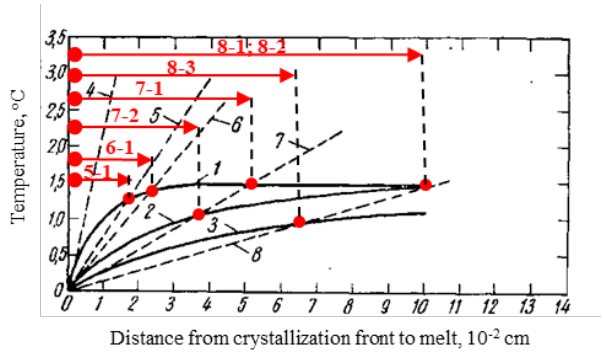

Fig. 2. The influence of the movement rate of the crystallization front (R) and the temperature gradient in the melt (G_L) (dashed lines 4-8) on the length of the concentration undercooling zone (red lines) before of the flat crystallization front at different values of the liquidus temperature (solid lines 1-3)
Line numbers: 1 – R = 1,7·10^{-2} cm/s; 2 - R = 5·10^{-3}; 3 - R = 2·10^{-3}; 4 – G_L = 498 K/cm; 5 – G_L = 348; 6 – G_L = 333; 7 – G_L = 303; 8 – G_L = 288.
The first number on the red line is G_L line number; Second – R.

Analysis of the data in Fig. 2 shows that depending of the movement speed of the crystallization front, the temperature gradient in the melt and the liquidus temperature, the extent of the

zone of concentration undercooling before of the flat crystallization front can change in ten times.

According work [13], the kinetics of undercooling (Δt) changes by chemical element ***i*** ahead of a growing dendrite is described by the following relationship:

$$\Delta t = \frac{G_i D_i}{R}, \tag{11}$$

The maximum undercooling (Δt_{max}) created by chemical element ***i*** ahead of the progressing flat crystallization front, according to the data of [14], is realized under the following condition:

$$\Delta t_{\max} = \frac{m_i C_{0i}(1-k_{ief})}{k_{ief}} - \frac{G_i D_i}{R} + \frac{G_i D_i}{R} \ln\left(\frac{G_i \cdot D_i}{R} \cdot \frac{k_{ief}}{m_i C_{0i}(1-k_{ief})}\right) \tag{12}$$

where: m_i is the tangent of the liquidus line slope; C_{0i} is the quantity of element ***i*** in the melt; k_{ief} – effective distribution coefficient of element *i*; D_i is the diffusion coefficient of element *i* in the melt; *R* - crystallization rate; G_i is the temperature gradient in the melt ahead of the crystallization front.

It is shown in [7, 11, 15, 16] that with the development of concentration undercooling ahead of a flat crystallization front, it subsequently transforms into cellular and dendritic. However, there are no quantitative regularities of the influence of concentration undercooling on the dendritic structure of steel castings.

Therefore, the purpose of this work is to study the influence of chemical composition and temperature on the development of concentration undercooling and the dendritic structure of structural steel castings and to determine the analytical dependence of such influence.

2. Methodology

Based on the analysis of the crystallization process, the main parameters were established that determine the conditions for maximum undercooling before the crystallization front. These include the ratio of the temperature gradient in the melt ahead of the crystallization front to the crystallization rate (G_i/R); tangent of the liquidus line (m_i); quantity of elements ***i*** in the melt (C_{0i}); equilibrium (k_{0i}) and effective (k_{ief}) distribution coefficient of elements ***i*** and diffusion coefficient of elements ***i*** in the melt. (D_i).

The influence of the chemical composition and steel temperature on the equilibrium and effective distribution coefficients of elements and their diffusion coefficient in the melt was determined by multiple correlation analysis of experimental data given in [17-22].

The numerical solution of the analytical dependences of the influence of the above factors on the effective distribution coefficient of elements and the maximum undercooling before the crystallization front was carried out from the condition of the minimum value of the difference between the left and right sides of the equations at four significant numbers of the factor being determined. The error in the numerical solution of the equations ranged from 0.003 to 0.159%

The adequacy of the calculations was checked using the example of castings from steels 20KhGSL and 40Kh3G3S3L. Steels were melted in IST 016 induction furnace with a basic lining with using industrial ferroalloys. The chemical composition of the steels was determined using an SPAS-05 optical emission spectrometer. The chemical composition of steels and liquidus temperatures are given in Table 1.

The castings were obtained by the investment casting at 1600 °C in ceramic molds. The scheme of casting and gating system is depicted in Figure 1 of work [23]. Diameter of casting – 20 mm, length – 150 mm. The distance from the axis of the riser to the place where the sample was cut was of 70 mm. The rate of castings crystallization was about $3 \cdot 10^{-4}$ m/s.

The columnar and equiaxed disoriented dendrite zones was investigated on longitudinal templates by etching in a reagent containing 10 ml HNO_3, 30 ml HCl at 100 °C during 10–15 s. Size of the columnar dendrites zone was studied using MIM-10 optical microscope.

Mathematical processing of the experimental data was carried out using the least squares method, with a probability of 95%.

Table 1.
The chemical composition and liquidus (t_l) temperatures of the cast steels

No.	Alloy grade	Content of elements, wt. %							t_l, °C
		C	Si	Mn	Cr	S	P	N	
1	20KhGSL	0.21	0.91	0.90	0.90	0.024	0.010	0.014	1504
2	40Kh3G3S3L	0.41	3.48	3.00	2.95	0.035	0.025	0.013	1443

3. Results and discussion

Analysis of the kinetics and conditions for the development of concentration undercooling (equations 11 and 12) shows that when maximum concentration undercooling is achieved, the following dependence is realized:

$$\left(\frac{G_i}{R}\right) \cdot \left(2 - \ln\left[\frac{D_i k_{ief}\left(\frac{G_i}{R}\right)}{m_i C_{0i}(1-k_{ief})}\right]\right) = \frac{m_i C_{0i}(1-k_{ief})}{k_{ief} \cdot D_i} \tag{13}$$

By solving equation (13) relatively to (G_i/R), can determine the critical value $(G_i/R)_{cr}$ at which the maximum possible undercooling for a given quantity of element ***i*** will be achieved. Work [11] shows that the G/R value for a metal containing several elements is determined as the sum of (G_i/R) for each element or impurity.

Having calculated the critical value $(G/R)_{cr}$ for a given chemical composition as

$$(G/R)_{cr} = \sum_{i=1}^{n} (G_i/R)_{cr} \tag{14}$$

it is possible to determine the conditions of maximum undercooling before the crystallization front.

Considering that during solidification of the casting $(G_i/R)_{cast}$ changes from maximum in the near-wall zone to minimum in the center of the casting [10, 24], the most favorable conditions for the nucleation and growth of equiaxed disoriented crystals before of the column dendrites front will be realized in the case when

$$(G/R)_{cast} = (G/R)_{cr} \tag{15}$$

At the same time, equality (15) will characterize the conditions for stopping of the column dendrites front, since it is know that its progress stops with the appearance of equiaxed disoriented crystals before of it. Consequently, by changing the value of $(G/R)_{cr}$) it is possible to predict a change in the size of the columnar dendrites zone, since a larger value of $(G/R)_{cr}$ should correspond to a smaller extent and vice versa (Fig. 3).

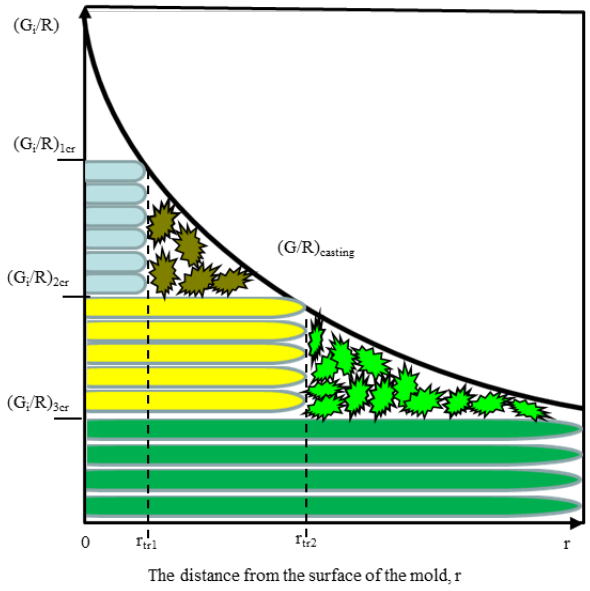

Fig. 3. Scheme for assessing of the influence of the parameter $(G_i/R)_{cr}$ on the size of the columnar dendrites zone in castings

For chemical compositions characteristic of structural steels, the values of the factors included in formula (13) were determined in order to numerically solve the equation.

The tangent of the liquidus line slope (m_i, °C/%) was determined by the formula that shows the influence of alloying elements on the liquidus temperature (t_l) of structural steels [25]

$$t_l = 1539 - 78\cdot[C] - 12\cdot[Si] - 5\cdot[Mn] - 1.5\cdot[Cr] - \\ - 25\cdot[S] - 30\cdot[P] - 2\cdot[V] - 90\cdot[N] \tag{16}$$

where: [C], [Si], [Mn], [Cr], [S], [P], [V], [N] content (wt. %) of carbon, silicon, manganese, chromium, sulfur, phosphorus, vanadium and nitrogen in the melt, respectively.

The influence of the chemical composition on the diffusion of elements in the melt was determined according to the data given in [20 - 22] (Table 2), which are components of the well-known diffusion Arrhenius equation [26]

$$\ln D_i = \ln D_o - Q/(RT) \tag{17}$$

where: D_o – pre-exponential factor, m^2/s; Q – activation energy of the diffusion process; R – universal gas constant.

Table 2.
Influence of chemical composition on the diffusion coefficient of C, Si, Mn, Cr (D_i, m^2/s) in melts of structural steels

Element	ln D_o	Q/R
C	-12.08-0.05C+0.202Si+0.033Mn+ +0.037Cr+0.066P+0.481S	-10885
Si	-9.28+0.245C+0.051Si+0.0046Mn+ +0.06Cr+0.203P+0.134S	-18688
Mn	-17.37+0.0049C+0.104Si-0.021Mn- 0.00535Cr	-2766
Cr	-15.717-0.131C+0.327Si-0.457Mn+ +0.158Cr+0.327 P+0.030 S	-7042
N	-18.2+0.163C-0.122Si-0.148Mn +0.065Cr+ +0.0476S+0.0744P	-1389
S	-40.8+0.234C+0.102Si--0.0585Mn- -0.0226Cr	39358
P	-77.94+0.106C+0.107Si-0.113Mn + +0.0825Cr	106484

Equation (13) includes the effective distribution coefficient (k_{ief}), which is related to the equilibrium (k_{i0}) as follows [11]:

$$k_{ief} = \frac{k_{i0}}{k_{i0} + (1 - k_{i0})\exp(-R\cdot\delta_i / D_i)} \tag{18}$$

where δ_i - the width of the melt zone before the crystallization front in which the redistribution of element ***i*** occurs as a result of diffusion.

The influence of chemical composition on the equilibrium distribution coefficient of elements between the liquid and solid phases was studied as follows. It is known [27-29] that the influence of the third element (**j**) in the **Fe – i – j** system on the equilibrium distribution coefficient of element **i** is determined by the following dependence:

$$\ln k_{0i}^{j} = \ln k_0^i + (\varepsilon_i^{i,l} - \varepsilon_i^{i,s}\cdot k_0^i)N_i^l + (\varepsilon_i^{j,l} - \varepsilon_i^{j,s}\cdot k_0^j)N_j^l \tag{19}$$

where: k_0^i, k_0^j - accordingly, the equilibrium distribution coefficients of elements **i** and **j** in binary systems **Fe – i** and **Fe - j**; $\varepsilon_i^{i,l}; \varepsilon_i^{i,s}; \varepsilon_i^{j,l}; \varepsilon_i^{j,s}$ - parameters of elements interaction **i** and **j** in liquid (l) and solid (s) metal; N_i^l, N_j^l - mole fractions of elements **i** and **j** in the melt.

In works [27,29] it was showen that the interaction parameters of elements in the melt ($\varepsilon_i^{i,l}; \varepsilon_i^{j,l}$) and solid iron ($\varepsilon_i^{i,s}; \varepsilon_i^{j,s}$) at the liquidus temperature are almost the same. For example, according [27], $\varepsilon_i^{C,s} = 0{,}925\varepsilon_i^{C,l}$, where i – Si, Ni, Mn, Mo, Cr, V. According to the work [29], $\varepsilon_C^{j,s} = 1{,}03\varepsilon_C^{j,l}$, where j – Co, Mn, Mo, Ti, W, V, Ta, Nb. The results of [31] show that $\varepsilon_C^{C,s} = 1{,}006\varepsilon_C^{C,l}$, where j – Si, Al, P, Ni, Cu, Mn, W, Mo, Cr, V.

The data presented confirm the correctness of the assumption made in [27,29] that at temperature the liquidus is $\varepsilon_i^{j,s} \approx \varepsilon_i^{j,l}$. This assumption allows us to propose, taking 1 % wt. of solution as the standard state, for dilute multicomponent iron-based systems the following relationship

$$\lg k_{0i}^j = \lg k_0^i + e_i^i(1-k_0^i)[i] + \sum_{i=1}^{n} e_i^j(1-k_0^j)[j] \qquad (20)$$

where: k_{0i}^j - equilibrium distribution coefficient of element **i** in a multicomponent iron-based system containing **j** elements; [**i**], [**j**] – wt. % of elements **i** and **j** in the melt; $e_i^i; e_i^j$ - parameters of element interaction **i** and **j** at liquidus temperature.

The temperature dependences of interaction parameters ($e_i^{i,j} = A/T + B$) for C, Si, Mn, Cr, S, P and N in multicomponent iron solutions are given in [19] (Table 3).

Table 3.

Temperature dependences of interaction parameters ($e_i^{i,j} = A/T + B$) [19]

Element, ***i***	Element, ***j***													
	C		Si		Mn		Cr		S		P		N	
	A	B	A	B	A	B	A	B	A	B	A	B	A	B
C	158	0.0581	162	0.008	-26.6	$2.18\cdot10^{-3}$	-56.4	$6.14\cdot10^{-3}$	49.8	$1.94\cdot10^{-2}$	49.8	$2.44\cdot10^{-2}$	100	$5.68\cdot10^{-2}$
Si	380	-0.023	34.5	0.089	3.32	$2.27\cdot10^{-4}$	-0.564	$1.42\cdot10^{-6}$	46.4	$3.12\cdot10^{-3}$	49.8	$3.13\cdot10^{-2}$	110	$3.15\cdot10^{-2}$
Mn	-149	$9.78\cdot10^{-3}$	0	0	0	0	7.3	$2.49\cdot10^{-4}$	-113	$1.23\cdot10^{-3}$	-6.6	$4.6\cdot10^{-5}$	3109	-1.83
Cr	-266	$2.18\cdot10^{-2}$	-8	$4.48\cdot10^{-5}$	6.97	$2.07\cdot10^{-4}$	-0.564	$1.42\cdot10^{-6}$	-153	0.062	-126	$1.44\cdot10^{-2}$	-498	$7.59\cdot10^{-2}$
S	133	$3.91\cdot10^{-2}$	53	$3.46\cdot10^{-2}$	-59.8	$5.91\cdot10^{-3}$	-94.2	0.0396	233	-0.153	-855	0.49	16.6	$1.13\cdot10^{-3}$
P	132	$5.91\cdot10^{-2}$	20.2	$5.33\cdot10^{-2}$	-76.4	$8.78\cdot10^{-3}$	-69.7	$7.23\cdot10^{-3}$	40	$6.72\cdot10^{-3}$	43.1	$3.9\cdot10^{-2}$	110	$3.55\cdot10^{-2}$
N	130	$5.90\cdot10^{-2}$	56.4	$1.68\cdot10^{-2}$	-43.2	$3.05\cdot10^{-3}$	-122.9	$1.86\cdot10^{-2}$	12.3	$4.4\cdot10^{-4}$	49.8	$1.84\cdot10^{-2}$	0	0

In work [11] it is shown that the width of the melt zone before of the crystallization front in which the redistribution of element ***i*** occurs as a result of diffusion is determined by the diffusion coefficient, crystallization rate and distribution coefficient. According to [11] accepted that

$$\delta_i = \frac{D_i}{k_{ief} \cdot R} \qquad (21)$$

where: $k_{ief} = k_0$ at the initial moment and $k_{ief} = 1$ at the final moment of crystallization.

Taking into account formulas (20) and (21), equation (18) can be written in the following form

$$k_{ief}^j = \frac{k_{0i}^j}{k_{0i}^j + (1-k_{0i}^j)\exp(-1/k_{ief}^j)} \qquad (22)$$

where: k_{ief}^j - effective distribution coefficient of element ***i*** in a multicomponent iron-based system containing **j** elements

The numerical solution of equation (22) makes it possible to determine the values of the effective distribution coefficient of elements in a multicomponent iron-based system depending of the value of the equilibrium coefficient.

The equilibrium distribution coefficients of elements in iron are given in Table 4.

Table 4.

Equilibrium distribution coefficients of elements in iron [18-20]

Kind of value	Elements	k_0 δ-Fe	k_0 γ-Fe	Elements	k_0 δ-Fe	k_0 γ-Fe
Min		0.11	0.30		0.60	0.50
Max	C	0.29	0.40	Si	0.85	0.61
Aver.		0.187	0.34		0.733	0.543
Min		0.89	0.85		0.68	0.70
Max	Cr	0.97	0.88	Mn	0.90	0.85
Aver.		0.933	0.865		0.781	0.77
Min		0.78	0.63		0.25	0.47
Max	V	0.96	0.63	N	0.38	0.50
Aver.		0.875	0.63		0.336	0.483
Min		0.02	0.01		0.13	0.06
Max	S	0.06	0.05	P	0.50	0.13
Aver.		0.0384	0.0263		0.191	0.085

The above calculations were verified on castings made from steels 20KhGSL and 40Kh3G3S3L, the chemical composition of

which is given in Table 1. Their average values during crystallization of γ-Fe were taken as the coefficients of equilibrium distribution of elements in iron. The results of calculating the parameters are shown in Table 5.

A comparison of the calculation results with experimental data shows that larger values of the $(G/R)_{cr}$ criterion correspond to a smaller width of the zone of columnar derdrites (Fig. 4).

Table 5.
Calculation of conditions for maximum concentration undercooling in steel castings 20KhGSL and 40Kh3G3S3L

Parameter	C	Si	Mn	Cr	S	P	N
	20KhGSL						
C_{oi}, wt. %	0.21	0.91	0.90	0.90	0.024	0.010	0.014
m_i, K/wt. %	78	12	5	1,5	25	30	90
D_i, m^2/s	$1.58\cdot10^{-8}$	$2.96\cdot10^{-9}$	$6.50\cdot10^{-9}$	$2.85\cdot10^{-9}$	$8.44\cdot10^{-9}$	$1.63\cdot10^{-8}$	$5.02\cdot10^{-9}$
k_0^i	0.340	0.543	0.770	0.865	0.0263	0.085	0.483
k_{0i}^j	0.389	0.644	0.749	0.824	0.0285	0.092	0.516
(k_{ief}^j)*	0.719	0.854	0.900	0.932	0.3460	0.465	0.791
$((G_i/R)_{cr})$*, K·s/m²	$1.288\cdot10^{8}$	$2.000\cdot10^{8}$	$2.442\cdot10^{7}$	$2.179\cdot10^{8}$	$4.270\cdot10^{7}$	$6.731\cdot10^{6}$	$2.108\cdot10^{7}$
Infuence of $(G_i/R)_{cr}$, %	20.1	31.2	3.8	34.0	6.6	1.0	3.3
$(G/R)_{cr} = \sum_{i=1}^{n}(G_i/R)_{cr}$	$6.416\cdot10^{8}$=100%						
	40Kh3G3S3L						
C_{oi}, wt. %	0.41	3.48	3.00	2.95	0.035	0.025	0.013
m_i, K/wt. %	78	12	5	1,5	25	30	90
D_i, m^2/s	$2.47\cdot10^{-8}$	$2.80\cdot10^{-9}$	$7.62\cdot10^{-9}$	$2.98\cdot10^{-9}$	$2.13\cdot10^{-8}$	$1.72\cdot10^{-7}$	$3.10\cdot10^{-9}$
k_0^i	0.340	0.543	0.770	0.865	0.0263	0.085	0.483
k_{0i}^j	0.523	0.926	0.733	0.781	0.0338	0.108	0.581
(k_{ief}^j)*	0.794	0.972	0.894	0.914	0.3600	0.486	0.824
$((G_i/R)_{cr})$*, K·s/m²	$1.068\cdot10^{8}$	$1.366\cdot10^{8}$	$7.419\cdot10^{7}$	$4.445\cdot10^{7}$	$2.321\cdot10^{7}$	$1.466\cdot10^{6}$	$2.562\cdot10^{7}$
Infuence of $(G_i/R)_{cr}$, %	25.9	33.1	18.0	10.8	5.6	0.4	6.2
$(G/R)_{cr} = \sum_{i=1}^{n}(G_i/R)_{cr}$	$4.123\cdot10^{8}$=100%						

*- relative error of the numerical solution of equation (13) from 0.003 to 0.159%; equation (22) from 0.007 to 0,143%

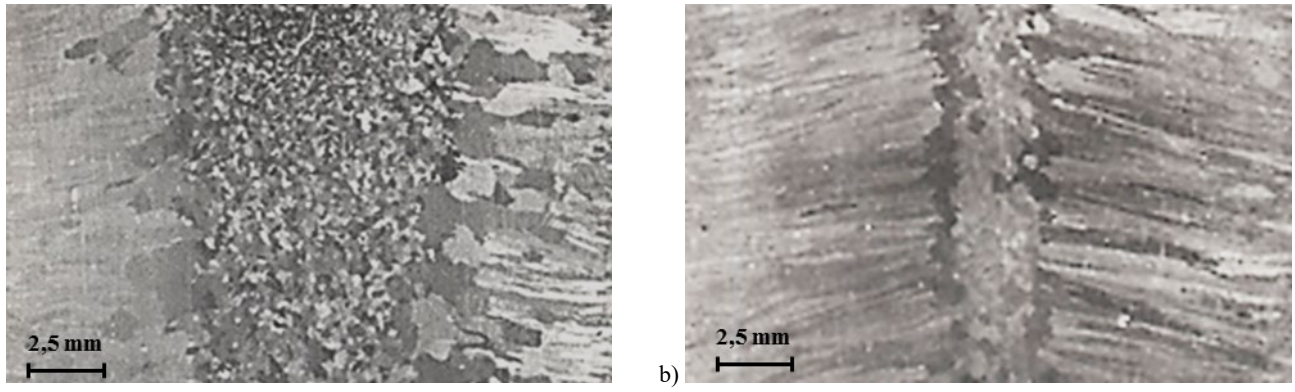

Fig. 4. Influence of the parameter $(G/R)_{cr}$ on the size of the columnar dendrite zone in steel castings 20KhGSL (a) and 40Kh3G3S3L (b). a - $(G/R)_{cr} = 6.416\cdot10^{8}$ K·s/m²; b - $(G/R)_{cr} = 4.123\cdot10^{8}$ K·s/m²

Analysis of the images shown in Fig. 4 shows that the length of the columnar dendrite zone in castings of 20KhGSL steel (Fig. 4 a) varies from 2.3 to 6.2 mm, and in castings made of

40Kh3G3S3L steel (Fig. 4 b) from 2.4 to 8.8 mm. Measurement (tolerance) error is of ± 2 μm [33]. The average values are of 4.7 and 7.9 mm, respectively. An increase of the $(G/R)_{cr}$ parameter from $4.123 \cdot 10^8$ K·s/m^2 to $6.416 \cdot 10^8$ K·s/m^2 leads to a decrease of the volume fraction of the columnar dendrite zone from 95.5% in castings made of 40Kh3G3S3L steel to 72.4% in castings made of 20KhGSL steel.

Analysis of the influence of elements on the values of the parameter $(G/R)_{cr}$ shows that the effectiveness of their influence on the maximum undercooling before the crystallization front significantly depends of the chemical composition and varies from 20.1 (steel 20KhGSL) to 25.9 (steel 40Kh3G3S3L)% for carbon, from 31.2 to 25.9% for silicon, from 3.8 to 18.0% for manganese, from 34.0 to 10.8% for chromium, from 6.6 to 5.6% for sulfur , from 1.0 to 0.4% for phosphorus, from 3.3 to 6.2% for nitrogen.

In steel 20KhGSL, depending on the increase in the degree of influence, the elements can be arranged in the following sequence: P, N, Mn, S, C, Si, Cr. In the case of steel 40Kh3G3S3L, a different sequence is observed: P, S, N, Cr, Mn, C, Si.

When the chemical composition of steel changes, there is a change of the liquidus temperature, diffusion mobility of elements and distribution coefficients, which can lead to both an increase and a decrease in the effectiveness of the influence of elements on maximum undercooling before the crystallization front.

The calculation results show that when the chemical composition of steel changes from 20KhGSL to 40Kh3G3S3L, the effectiveness of the influence of silicon increases on 6%, carbon - 29%, nitrogen - 1.9 times, and manganese - 4.7 times. At the same time, there is a decrease of the sulfur influence on 15%, phosphorus - 60% and chromium - 68%.

The results of the conducted research can be used to improve the quality of cast steel blanks by purposefully changing the width of the columnar dendrite zone. For example, in [30] it is shown that with a 19% decrease of the columnar dendrite zone, the axial liquation in a cast steel blank decreases by 18%. The expansion of the equiaxed crystal zone ensures a more uniform distribution of sulfides, non-metallic inclusions and other liquates over the cross-section of the blank, which significantly improves the quality of the axial zone and increases the impact toughness and reduction of area of steel [31]. In [32] it is shown that the expansion of the equiaxed crystal zone leads to an increase in the tensile strength and yield strength of steel from 4 to 5% and from 3 to 6%, respectively, and the relative elongation from 10 to 13%.

4. Conclusions

Considering that the equations describing such defining parameters of crystallization as the rate of nucleation of centers and the linear rate of crystallization include the undercooling of the melt around the particles of the solid phase, the influence of the chemical composition of structural steels on it was studied.

By analyzing of concentration undercooling, an analytical dependence has been established that allows us to determine the conditions for the development of maximum concentration undercooling ahead of the moving crystallization front depending of the liquidus temperature, element content in the melt, distribution and diffusion coefficients of elements, crystallization rate and temperature gradient in the melt before the crystallization front.

For structural steels, a correlation has been established between the width of the zone of columnar dendrites and the value of maximum concentration undercooling.

It is shown that the effectiveness of the influence of elements on the maximum undercooling before the crystallization front significantly depends of the chemical composition and varies, for the studied steels 20KhGSL and 40Kh3G3S3L, respectively, from 20.1 to 25.9% for carbon, from 31.2 to 25. 9% for silicon, from 3.8 to 18.0% for manganese, from 34.0 to 10.8% for chromium, from 6.6 to 5.6% for sulfur, from 1.0 to 0.4% for phosphorus, from 3.3 to 6.2% for nitrogen.

It has been established that when the chemical composition of steel changes, as a result of changes of the liquidus temperature, diffusion mobility of elements and distribution coefficients, both an increase and a decrease of the effectiveness of the element influence on maximum undercooling before the crystallization front can occur.

It is shown that when the chemical composition of steel changes from 20KhGSL to 40Kh3G3S3L, the effectiveness of silicon the influence increases on 6%, carbon - 29%, nitrogen in 1.9 times, manganese in 4.7 times and the influence of sulfur decreases on 15%, phosphorus - 60% and chromium - 68%.

References

[1] Gibbs, W. (1950). *Thermodynamic works.* Moscow: Nauka. (In Russian).

[2] Volmer, M. (1939). *Kinetik der Phasenbildung*. Dresden, Leipzig: Steinkopf.

[3] Sally, I. (1974). *Crystallization of alloys*. Kyiv: Naukova Dumka.

[4] Frank, F. (1949). The influence of dislocations on crystal growth. *Discusion of the Faraday Society*. *5*, 48-54.

[5] Turnbull, D. & Fisher, J.C. (1949). Rate of Nucleation in Condensed Systems. *Journal of Chemical Physics.* 17(1), 71-73.

[6] Volmer, M. & Marder, M. (1931). Zur Theorie der linearen Kristallisationsgeschwindigkeit unterkühlter Schmelzen und unterkühlter fester Modifikationen. *Zeitschrift für Physikalische Chemie A*, *154A*(1), 97–112. https://doi.org/10.1515/zpch-1931-15405. (in German)

[7] Flemings, M. (1974) Solidification processing. *Metallurgical Transactions. 5(10)*, 2121–2134. https://doi.org/10.1007/BF02643923.

[8] Hilling, W. & Turnbull, D. (1956). Theory of crystal growth in undercooled pure liquids. *Journal of Chemical Physics. 24(4),* 914. https://doi.org/10.1063/1.1742646.

[9] Turnbull, D. (1949) *Thermodynamics in Metallurgy*, ASM, Metals Park, Ohio.

[10] Efimov, V., Eldarkhanov, A. (2004). *Technologies of modern metallurgy.* Moskva: Novye tehnologii. (in Russian)

[11] Chalmers, B. (1968). *Principles of Solidification*. New-York-London-Sydney: John Wiley & Sons, Inc.

[12] Tiller, W. A., Jackson, K. A., Rutter, J. W. & Chalmers, B. (1953). The redistribution of solute atoms during the solidification of metals. *Acta Metallurgica.* 1, 428–437.
[13] Biloni, H., & Boettinger, W. J. (1996). Solidification. In R. W. Cahn & P. Haasen (Eds.), *Physical Metallurgy* (4th ed., pp. 669–842). Elsevier Science B.V.
[14] Timofeev, G. (1977). *Mechanics of alloys during crystallization of ingots and castings.* Moskva: Metallurgy
[15] Winegard, W. (1964). *An introduction to the solidification of metals*. London: The institute of metals.
[16] Kurz, W., Bezençon, C., & Gäumann, M. (2001). Columnar to equiaxed transition in solidification processing. *Science and Technology of Advanced Materials*. 2(1), 185-191. https://doi.org/10.1016/S1468-6996(01)00047-X.
[17] Ono, A. (1980). *Solidification of metals*. Moscow: Metallurgy.
[18] Hein, K., Buriga. E. (1987). *Crystallization from melts*. Handbook. Moscow: Metallurgy.
[19] Aftandilyants, E., Babaskin, Yu. (1995). Modeling of the process of dendritic structure formation in structural steel castings. *Casting processes (Procesy litya)*. 4, 94-106. (in Russian).
[20] Lepinskikh, B., Kaybichev, A., Savelyev, Y. (1974). *Diffusion of elements in liquid metals of the iron group*. Moscow: Nauka.
[21] Ershov, G., Mayboroda, V. (1990). *Diffusion in metal melts*. Kyiv: Naukova Dumka.
[22] Aftandilyants, E. (2019). Phase transformations of austenitic stainless modified steels. *The Scientific Technical journal Metal Science and Treatment of Metals*. *25*, 2. 11-17. https://doi.org/10.15407/mom2019.02.011
[23] Aftandiliants, Y., Gnyloskurenko, S., Meniailo, H. & Khrychikov, V. (2024). Influence of melt properties on the dendritic structure of steel castings. *Archives of Foundry Engineering*. *24(1),* 5-14. DOI: 10.24425/afe.2024.149245.
[24] Golod, V. M. & Orlova, I. G. (2012). Analysis of structural microheterogeneity of low-carbon steels based on computer modeling of their solidification conditions. *Scientific and Technical Statements of SPbSPU. Series "Science and Education"*. 2012(1), 177–182. (in Russian).
[25] Denisov, V.A. & Denisov, A.V. (1983). Method of calculation of solidification temperatures of steel. *Foundry production (Liteynoye proizvodstvo)*. 5*,* 11. (in Russian)
[26] Van Vlack, H. (1975). *Materials Science for engineers*. California-London-Ontario: Addision –Wesley Publishing company.
[27] Morita, Z. & Tanaka, T. (1983). Thermodynamics of Solute Distributions between Solid and Liquid Phases in Iron-base Ternary Alloys. *Transactions of the Iron and Steel Institute of Japan.* 23(10), 824-833. https://doi.org/10.2355/isijinternational1966.23.824
[28] Shmigra, L. (1985). *Crystallization and solidification of steel ingots.* Moscow: Metallurgiya. (in Russian).
[29] Morita, Z. & Tanaka, T. (2003). Thermodynamics of Equilibrium Distribution of Solute Elements in Solidification Process of Steel. *High Temperature Materials and Processes*. 22(5-6), 329-336.
[30] Parusov, E.V., Sychkov, O.B., Gubenko, S.I., Sagura, L.V. (2016). Influence of chemical composition and dendritic structure of continuously cast billets on the appearance of liquation phenomena in bundle rolled products. *Reporter of the Priazovskyi state technical university. Series: Technical sciences.* 32, 61-71. (in Ukrainian) http://nbuv.gov.ua/UJRN/vpdty_2016_32_11
[31] Kazachkov, E.A., Fedosov, A.V. (2006). Peculiarities of axial liquation formation in continuous cast slab. *Bulletin of the Azov State Technical University. Series: Technical sciences.* 16, 1-5.
[32] Gubenko, S.I. (2015). *Non-metallic inclusions and strength of steels. Palmarium Academic Publishing*. Deutschland (In Russian).
[33] Metallographic. microscope MIM-10. (2024). Technical characteristics. Retrieved January 17, 2025, from https://asma.net.ua/uk/p/1464605834-mikroskop-mim-10-metallograficheskiy/